Gαo Represses Insulin Secretion by Reducing Vesicular Docking in Pancreatic β-Cells

Aizhen Zhao,[1] Mica Ohara-Imaizumi,[2] Marcella Brissova,[3,4,5] Richard K.P. Benninger,[3] Yanwen Xu,[1] Yuhan Hao,[1] Joel Abramowitz,[6] Guylain Boulay,[7] Alvin C. Powers,[3,4,5] David Piston,[3] Meisheng Jiang,[8] Shinya Nagamatsu,[2] Lutz Birnbaumer,[6] and Guoqiang Gu[1]

OBJECTIVE—Pertussis toxin uncoupling–based studies have shown that Gαi and Gαo can inhibit insulin secretion in pancreatic β-cells. Yet it is unclear whether Gαi and Gαo operate through identical mechanisms and how these G-protein–mediated signals inhibit insulin secretion in vivo. Our objective is to examine whether/how Gαo regulates islet development and insulin secretion in β-cells.

RESEARCH DESIGN AND METHODS—Immunoassays were used to analyze the *Gαo* expression in mouse pancreatic cells. *Gαo* was specifically inactivated in pancreatic progenitor cells by pancreatic cell–specific gene deletion. Hormone expression and insulin secretion in response to different stimuli were assayed in vivo and in vitro. Electron microscope and total internal reflection fluorescence–based assays were used to evaluate how Gαo regulates insulin vesicle docking and secretion in response to glucose stimulation.

RESULTS—Islet cells differentiate properly in $Gαo^{-/-}$ mutant mice. *Gαo* inactivation significantly enhances insulin secretion both in vivo and in isolation. *Gαo* nullizygous β-cells contain an increased number of insulin granules docked on the cell plasma membrane, although the total number of vesicles per β-cell remains unchanged.

CONCLUSIONS—Gαo is not required for endocrine islet cell differentiation, but it regulates the number of insulin vesicles docked on the β-cell membrane. ***Diabetes*** **59:2522–2529, 2010**

From the [1]Program in Developmental Biology and Department of Cell and Developmental Biology, Vanderbilt University Medical Center, Nashville, Tennessee; the [2]Department of Biochemistry, Kyorin University School of Medicine Mitaka, Tokyo, Japan; the [3]Department of Molecular Physiology and Biophysics, Vanderbilt University Medical Center, Nashville, Tennessee; the [4]Division of Diabetes, Endocrinology, and Metabolism, Department of Medicine, Vanderbilt University Medical Center, Nashville, Tennessee; the [5]VA Tennessee Valley Healthcare System, Nashville, Tennessee; the [6]Transmembrane Signaling Group, Laboratory of Neurobiology, National Institute of Environmental Health Sciences, National Institutes of Health, Department of Health and Human Services, Research Triangle Park, North Carolina; the [7]Department of Pharmacology, School of Medicine, Sherbrooke University, Sherbrooke, Québec, Canada; and the [8]Department of Molecular and Medical Pharmacology, University of California, Los Angeles, Los Angeles, California.

Corresponding author: Guoqiang Gu, guoqiang.gu@vanderbilt.edu.

Received 23 November 2009 and accepted 1 July 2010. Published ahead of print at http://diabetes.diabetesjournals.org on 9 July 2010. DOI: 10.2337/db09-1719.

Nutritional signals, including glucose and amino acids, are the major inducers for insulin secretion in pancreatic β-cells. Upon glucose entry into β-cells, glucokinase initiates glucose metabolism to increase the cytosolic ATP/ADP ratio (1). Increase in the ATP/ADP ratio leads to closure of K_{ATP} channels and membrane depolarization, which in turn opens voltage-gated calcium channels and causes increases of intracellular calcium, triggering insulin secretion (2). Neuronal and hormonal signals modulate secretion in response to nutrients by modifying the activity and effects of secondary messengers or effector molecules that control secretion (3–5).

Heterotrimeric G-protein (Gαβγ) coupled receptors are the major mediators of hormonal and neuronal signals in modulating insulin secretion (6,7). Neurotransmitters or neuropeptides bind their respective receptors to activate the G-proteins, which subsequently transmit regulatory signals by modifying the production of secondary messengers or interacting with effector molecules. All G-protein subunits can transmit signals (8), with Gα being the major determinant of the specificity and strength of signaling (8,9). There are four subfamilies of Gα proteins (Gαs, Gαq/11, Gα12/13, and Gαi/o). All of these subfamily members are expressed in β-cells and are thought to be involved in insulin secretion regulation. For example, cholecystokinin, glucagon, glucagon-like peptide-1, and PACAP activate Gαs to stimulate adenosine cAMP production and potentiate insulin secretion through protein kinase A–dependent and –independent (i.e., cAMP-GEFII) pathways. In contrast, galanin, somatostatin, and adrenaline activate Gαi/o proteins to inhibit insulin secretion through both calcium-dependent and -independent processes (10). The presence of these different mechanisms highlights the diverse roles and functions of G-proteins in regulating insulin secretion.

The collective roles of Gαi/o proteins in insulin secretion have long been established. Pertussis toxin (or islet-activating protein, [PTX]) ADP-ribosylates Gαi/o proteins to release the inhibitory effect of adrenaline on insulin secretion through Gαi/o-coupled receptors (11–13). However, because PTX modifies Gαi1, Gαi2, Gαi3, and Gαo simultaneously, the individual in vivo function of each of these G-proteins is not clear; whether they function through a common mechanism is also unclear (14).

Gαo, the most abundant G-protein in neuronal and neuroendocrine cells, produces two protein isoforms: Gαo1 and Gαo2, through two alternatively spliced mRNAs (15,16). The in vivo inhibitory mechanism of Gαo on insulin secretion remains largely unclear due to the possible redundancy among the Gαi/o proteins as well as a lack

of loss-of-function studies in vivo. One possible mechanism is that Gαo regulates vesicle docking or the vesicle/cytoplasmic membrane fusion process. This above hypothesis is in line with some recent findings that show the Gβγ complex can directly interact with the SNARE complex in neuroendocrine cells (17–19) to modulate secretion. Whether Gαo inhibits insulin secretion through such a mechanism (e.g., Gαo regulates the intracellular Gβγ concentration by sequestration in response to hormone stimulation) has not been investigated as of yet.

Gαo$^{-/-}$ null mice displayed severe physiological defects such as compromised viability, shortened life span, reduced body weight, defects in pain perception, and defects in movement (tremors and seizures) (20,21). Thus, characterization of their islet phenotype was hindered by these pleiotropic defects. Here, we used tissue-specific loss of function in the mouse to analyze the function of Gαo specifically in islet cells. We show that *Gαo*-deficient β-cells have a significant increase in cell membrane–docked insulin vesicles as compared with control cells. These findings suggest that Gαo functions as a repressor of insulin secretion by delaying the vesicle docking/priming process, either directly or indirectly, in β-cells.

RESEARCH DESIGN AND METHODS

The *Pdx1*^{Cre} allele was described previously (22). The derivation of *Gαo*^{F} will be described elsewhere (M.J., L.B., unpublished data).

Immunofluorescence/immunohistochemistry and RT-PCR followed established protocols. Mouse anti-Gαo was a gift from R. Jahn (23). Guinea pig anti-insulin, guinea pig anti-glucagon, guinea pig anti-pancreatic polypeptide, and rabbit anti-somatostatin were obtained from Dako, Carpinteria, CA. Mouse monoclonal anti-insulin antibody was purchased from Sigma-Aldrich, St. Louis, MO. Secondary antibodies used were fluorescein isothiocyanate–conjugated donkey anti-rabbit IgG; fluorescein isothiocyanate–conjugated donkey anti-guinea pig IgG; and Cy3-conjugated donkey anti-mouse IgG (Jackson Immunoresearch, West Grove, PA). Goat anti-mouse IgG conjugated to Alexa Fluor 488 was from Invitrogen, Carlsbad, CA. All antibodies were used at a 1:500–1:2,000 dilution. Oligos used for *Gαo* RT-PCR are as follows (Fig. 2): P1, 5′-cactgagcaggacatcctccga-3′; P2, 5′-catcctcaaagcagtggatcca-3′; P3, 5′-cttcctcaacaagaaagacctct-3′; P4, 5′-ggtgagcggtttttgctttcaaa-3′; P5, 5′-ca agtggttcacagacacatcta-3′; P6, 5′-ccttggatgtgagccacagct-3′. Oligos used for insulin expression assays are as follows: 5′-cagcaagcaggtcattgttt-3′ and 5′-gggaccacaaagatgctgtt-3′.

For β-cell mass assay, pancreata were weighed and cut as 20-μm frozen sections. One-tenth of the sections were randomly collected and stained for insulin expression. Confocal images (covering ~1/5 of all stained pancreatic areas) were randomly captured using a ×5 objective lens and analyzed with Bioquant software (24) to calculate the area ratio between β-cells and the whole pancreas to calculate islet mass.

Intraperitoneal PTX injection (at 1 μg/100 g body wt), intraperitoneal glucose tolerance test (IPGTT), insulin sensitivity assays, and serum insulin assays followed published procedures (25,26). Islet isolation and perifusion followed an established protocol (27). For cAMP assays, 12 animals of each genotype were used to prepare eight independent batches of islets. Islets were incubated in Ringer's solution (with 2 mmol/l glucose) with 0.1 mmol/l isobutylmethylxanthine (IBMX) for 2 h and then used for assaying cAMP levels with the cAMP Biotrak enzyme immunoassay system (GE Healthcare).

For perifusion, islets of similar size and shape were used. Hand-picked islet cells were isolated and placed in a 1-ml perifusion chamber, equilibrated in 5.6 mmol/l glucose for 30 min and then challenged with 16.7 mmol/l glucose (16.7 mmol/l glucose + 100 μmol/l IBMX), 300 μmol/l tolbutamide, and 20 mmol/l KCl. The perifusion fractions were collected in 3-min intervals at 1 ml/min flow rate and assayed for insulin by radioimmunoassay.

Fluorescent images were obtained using confocal microscopy (Zeiss LSM 510 inverted microscope). For transmission electron microscopy (TEM), islets were first isolated from six animals and fixed (0.25% gluteraldehyde in PBS) for sectioning and imaging. For quantification of vesicles docked on the cell membrane, images were captured using TEM at magnification ×10,000–15,000. The number of docked vesicles was counted before genotype identification, with vesicles whose outer surface was within 10 nm of the plasma membrane as docked granules. At least 50 randomly captured microscopic fields (from different β-cells) of each genotype were analyzed before identifying their genotype. For calcium imaging, a series of images were acquired from isolated islets under glucose levels of 2, 4, 6, 8, 10, and 15 mmol/l. Images were background subtracted, and the mean Fluo-4/Fura-Red intensity ratio was calculated across the whole islet (28). This ratio was then normalized to the ratio calculated at 4 mmol/l glucose stimulation.

Total internal reflection fluorescence microscopy (TIRFM)-based live cell imaging followed published procedures (29,30). Briefly, islets were isolated and dispersed in calcium-free Krebs-Ringer buffer (KRB) containing 1 mmol/l EGTA and cultured on high refractive index cover glass (Olympus) in RPMI medium. β-Cells were then infected with recombinant adenovirus Adex1CA insulin-green fluorescent protein (GFP) (29) for observation in KRB containing 2.2 mmol/l glucose (37°C). The Olympus TIRFM system was used with a high-aperture objective lens to observe the fluorescence of GFP with a charge-coupled device camera at 300-ms intervals using Metamorph version 7.1 (Universal Imaging). Stimulation with glucose was achieved by the addition of 52 mmol/l glucose–KRB into the chamber for a final concentration of 22 mmol/l glucose. Diiodomethane sulfur immersion oil (n = 1.81, Cargille Laboratories) was used to make contact between the objective lens and the high refractive index cover glass. Light propagates through the cover glass at an angle of 65° and undergoes total internal reflection at the glass–cell interface. The refractive indexes for the glass (n = 1.8 at 488 nm) and cells (n = 1.37) predict an evanescent field decline of threefold within 44 nm from the interface and of 10-fold within 100 nm. Most analyses, including tracking (single projection of different images) and area calculations were performed using Metamorph software, added with manual event selection. In this evanescent field setting, a granule would have a vertical distance of 9.6 nm from the plasma membrane and qualify as a morphologically docked granule (granule distance from plasma membrane <10 nm in electron microscopic studies) (31). We immunostained endogenous insulin granules in fixed pancreatic β-cells. Then, we manually counted bright spots as the docked granules.

All statistical analyses used the Student t test. A P value $\leq$ 0.05 was considered statistically significant. Quantified data are presented as mean ± SE.

RESULTS

Gαo is expressed in all endocrine islet cells. We examined Gαo protein expression in both embryonic and adult pancreata using a monoclonal antibody that recognized both Gαo1 and Gαo2. Robust Gαo production is detected in all hormone-expressing cells in all stages examined, including E11.5, E17.5, and 3-month-old adults (Fig. 1). We do not detect Gαo in exocrine acinar or pancreatic duct cells (Fig. 1 and data not shown). Further RT-PCR analyses showed that both *Gαo1* and *Gαo2* mRNA could be detected in adult islet cells, suggesting that both isoforms might be involved in islet cell function (Fig. 2*A* and *B*).

Gαo is not required for endocrine islet cell differentiation. We used a *Gαo* conditional allele, in which two LoxP sites flanked the fifth and sixth exons of *Gαo*, common to *Gαo1* and *Gαo2* (*Gαo*^{F}, Fig. 2*A*), to examine its role in β-cell function. Deletion of the flanked exons produces a truncated mRNA that only codes for the NH_2-terminal 156 amino acids, which lacks all motifs that bind to adenylyl cyclase, phospholipase Cs (PLCs), and the βγ subunits. We expect that this above manipulation results in a null *Gαo* allele (*Gαo*$^{-}$). Indeed, *Gαo*$^{-/-}$ animals display identical phenotypes as previously reported for null mutants (data not shown), whereas *Gαo*$^{+/-}$ mice showed a similar phenotype as wild-type littermates. Furthermore, the truncated protein did not perturb insulin secretion in a cultured β-cell line (supplementary Fig. 1, available in an online appendix at http://diabetes.diabetesjournals.org/cgi/content/full/db09-1719/DC1).

Gαo$^{F/F}$;*Pdx1*^{Cre} (*F/F;Cre*) adult animals were derived from standard genetic crosses. *Pdx1*^{Cre} animals express *Cre* in all undifferentiated pancreatic progenitors and inactivate *Gαo* in all pancreatic progenitor cells of *F/F;Cre* mice. This allows us to examine whether *Gαo* plays a role in islet cell development. In addition, no *Cre* toxicity in

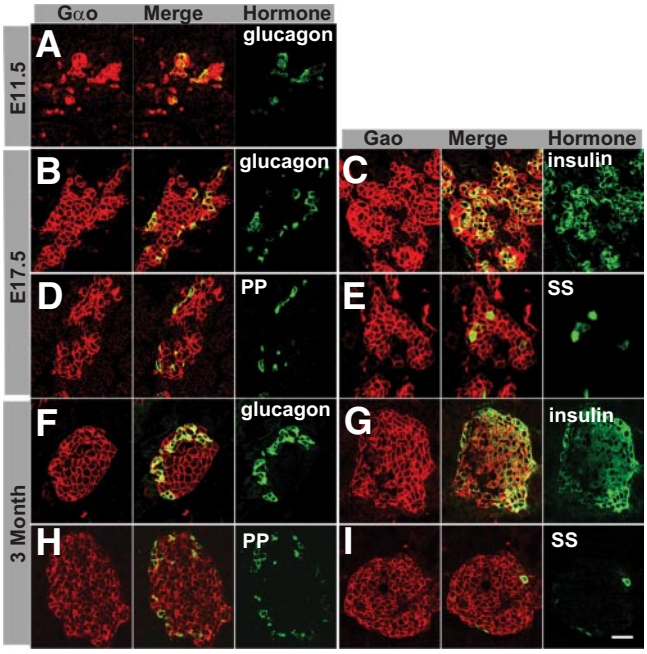

FIG. 1. *Gαo* is expressed in the endocrine islet cells of the pancreas. Expression patterns at three mouse stages, E11.5 (*A*), E17.5 (*B–E*), and 3-month-old adult (*F–I*), are shown. Immunofluorescence was used to visualize coexpression of *Gαo* with each endocrine hormone. Three panels: Gαo, hormone (*green*), and a merged image. Note that all hormone-expressing cells express Gαo. Scale bar = 20 μm. PP, pancreatic polypeptide; SS, somatostatin. (A high-quality digital representation of this figure is available in the online issue.)

Pdx1^{Cre} animals has been observed (22). RT-PCR assays showed that the mRNA sequence corresponding to the fifth and sixth exons of *Gαo* was no longer detectable in islets of 4-month-old *F/F;Cre* animals (Fig. 2*B*), confirming the effectiveness of *Pdx1*^{Cre} for *Gαo*^{F} deletion.

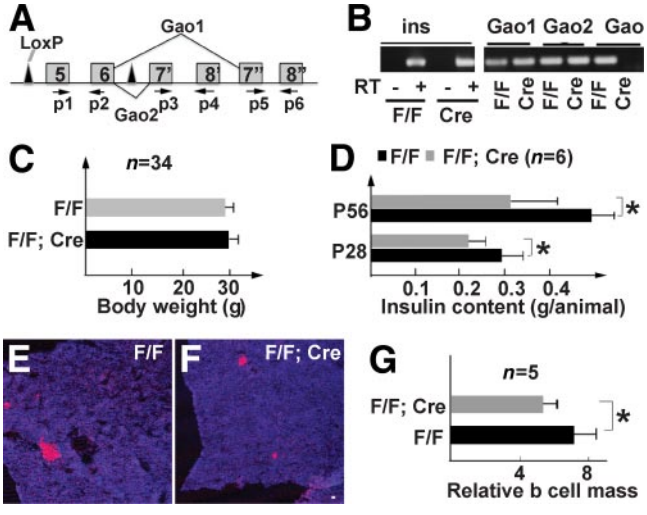

FIG. 2. *Gαo* is not required for islet cell differentiation. *A*: A diagram showing the *Gαo*^{F} (*F*) allele. Only some exons are shown (from 5 to 8). Exons 7′ and 8′ are specific to *Gαo2*. Exons 7′′ and 8′′ are specific to *Gαo1*. Arrows P1–P6 indicate the oligonucleotides used for detecting *Gαo* mRNAs in *B*, which shows RT-PCR detection of *Gαo* mRNA in 4-month-old adult islet cells. RT reactions with insulin-specific oligos were used as controls (with or without reverse transcription). (P5 + P6) detects *Gαo1* mRNA. (P3 + P4) detects *Gαo2* mRNA (Cre refers to *Gαo*$^{F/F}$*; Pdx1*^{Cre}). (P1 + P2) detects both *Gαo1* and *Gαo2* messages. *C*: Body weights of *F/F* and *F/F;Cre* animals at 12 weeks of age. *D*: Total insulin content in 4- and 8-week-old mice (P28 and P56). *E* and *F*: Insulin staining (*red*) in P56 pancreata. Topro3 (*blue*) highlights all pancreatic tissues. Scale bar = 50 μm. *G*: β-Cell mass in P56 animals. **P* < 0.05. (A high-quality color representation of this figure is available in the online issue.)

The *F/F;Cre* animals were no different in body weight from their control littermates (*Gαo*$^{F/F}$ or *F/F*) at all ages examined: 6, 9, 12, and 20 weeks (Fig. 2*C*). Additionally, no structural or behavioral (aggression, feeding, moving, and mating) defects were obvious in these animals. At postnatal day 1 (P1), the insulin contents in *F/F;Cre* and *F/F* pancreata were not significantly different (supplementary Fig. 2*A*, available in an online appendix), suggesting that Gαo is not required for β-cell differentiation. By P28, the insulin content in *F/F;Cre* animals was reduced by 20% over that of control littermates (Fig. 2*D*). At P56 (8 weeks), the insulin content of *F/F;Cre* animals had a 38% reduction compared with control littermates (Fig. 2*D*). Consistent with this finding, the β-cell mass was reduced in *F/F;Cre* animals at P56 as well (Fig. 2*E–G*). The reason for this reduction in insulin content is not currently clear.

We analyzed islet morphology and expression of several genes that are required for endocrine islet cell differentiation and function, including *MafA*, *MafB*, *Myt1*, *Nkx6.1*, and *Pdx1* (25) by immunofluorescence. None of the above markers were affected by *Gαo* inactivation (supplementary Fig. 2*B* and data not shown). These data suggest that *Gαo* is not required for islet neogenesis, even though it is expressed in early *Ngn3*-expressing endocrine progenitor cells (32).

Gαo is the major mediator of PTX's effect on insulin secretion inhibition. Gαi and Gαo inactivation by PTX uncouples the inhibitory effects of some neural hormones, such as adrenaline, on insulin secretion (12). Because both Gαi and Gαo are expressed in islet cells and they both can be ADP-ribosylated by PTX (14,33,34), it is not clear which G-protein is mediating the PTX effect on insulin secretion. We used the *Gαo* mutant allele to directly investigate this question.

The fasting blood glucose levels in *F/F;Cre* and *F/F* animals were similar (Fig. 3*A*, note the data points at 0 min). However, IPGTT showed that *F/F;Cre* animals have significantly improved glucose clearance over control littermates (Fig. 3*A*). Consistent with this observation, the fasting serum insulin levels are similar between *F/F* and *F/F;Cre* animals. Fifteen minutes after glucose challenge, the serum insulin levels in *F/F* control animals increased by 2-fold but increased up to 10-fold in *F/F;Cre* mice (Fig. 3*B*). Because the insulin sensitivity in *F/F;Cre* and control animals was similar (Fig. 3*C*), the above findings demonstrate that losing *Gαo* potentiates insulin secretion from β-cells. We next tested whether Gαi proteins function to repress insulin secretion in the absence of Gαo. If they do, we expect that PTX treatment of *F/F;Cre* animals would further potentiate insulin secretion. PTX injection into *F/F* animals resulted in a significant increase in glucose tolerance. Whereas PTX injection into *F/F;Cre* animals had no significant effect (Fig. 3*D*), suggesting that although Gαi proteins are expressed in islet cells and may be ADP-ribosylated by PTX, Gαo is the major mediator of PTX's effect on insulin secretion.

Gαo regulates insulin secretion at steps shared by different secretagogues. Islet perifusion assays were used to directly test how *Gαo* inactivation affects insulin secretion in vitro. Islets from 2-month-old animals were assayed for insulin secretion in response to glucose, IBMX, tolbutamide, and KCl stimulation. Glucose induces insulin secretion through metabolism to alter the ATP/ADP ratio and other metabolites. IBMX inhibits cAMP phosphodies-

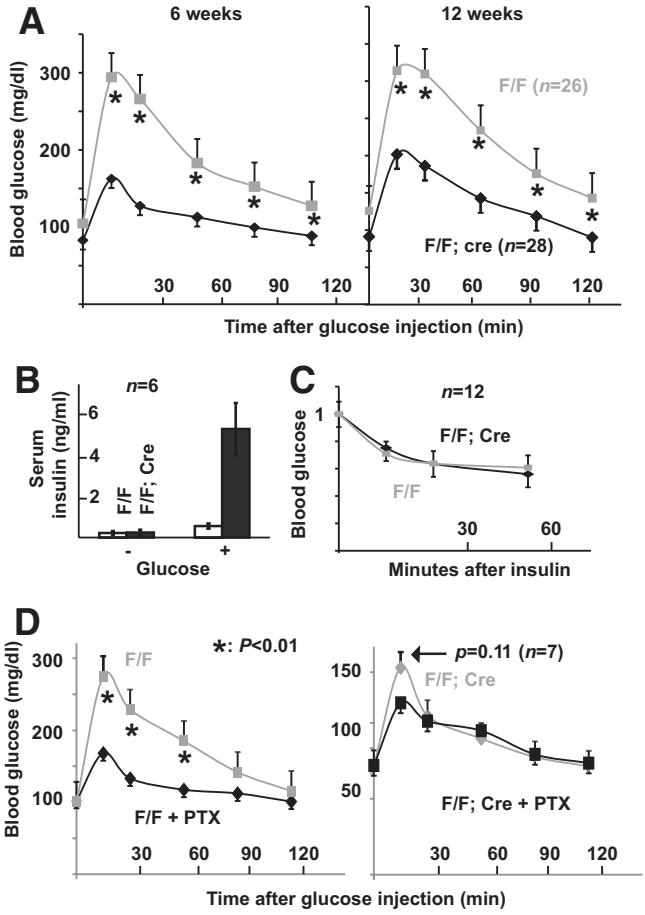

FIG. 3. Pancreas-specific *Gαo* inactivation enhances glucose-clearing capability in adult animals. *A*: IPGTT results in 6- and 12-week-old animals. *Gαo*$^{F/F}$;*Pdx1*^{Cre} (*F/F;Cre*) and *Gαo*$^{F/F}$ (*F/F*) animals were used. At least 13 males and 13 females of each genotype were assayed. Presented are the combined results from both males and females. *B*: Serum insulin levels 0 and 15 min after intraperitoneal glucose injection in 12-week-old *F/F;Cre* and *F/F* males. Note the fold increases in both control (gray bars) and *F/F;Cre* (black bars) animals after glucose stimulation. *C*: Insulin sensitivity of 12-week-old *F/F;Cre* and *F/F* animals. The *y*-axis is presented as the ratio of glucose levels of the assay point over that of the 0-min value. *D*: IPGTT results in animals treated with PTX. *$P < 0.01$.

terase to upregulate the levels of cAMP, which activates protein kinase A and/or GEFII to facilitate insulin vesicle exocytosis (35,36). Tolbutamide, a K_{ATP} channel blocker, depolarizes β-cell membrane potential, as does KCl. In response to these stimuli, the insulin secretion in the *F/F;Cre* islets was substantially increased compared with that of control littermates at every time point examined (Fig. 4*A*). The biggest increase was in response to glucose, increasing as much as 369% (Fig. 4*B*). This secretion increase was lower than what was detected during in vivo glucose challenge (Fig. 3*B*), likely due to the synergetic effect of multiple hormones that regulate insulin secretion through Gαo in vivo, but not in vitro. Importantly, these data suggest that Gαo regulates insulin secretion through a mechanism that is shared by all these stimuli, most likely in steps that are distal to Ca^{2+} mobilization, as suggested for in vitro–based studies (10).

Indeed, inactivation of *Gαo* did not significantly affect cAMP production in isolated islets (Fig. 4*C*). In addition, similar increases in intracellular free calcium ($[Ca^{2+}]_i$) concentration were seen in both *F/F;Cre* mutant and control islets after elevated glucose stimulation (Fig. 5).

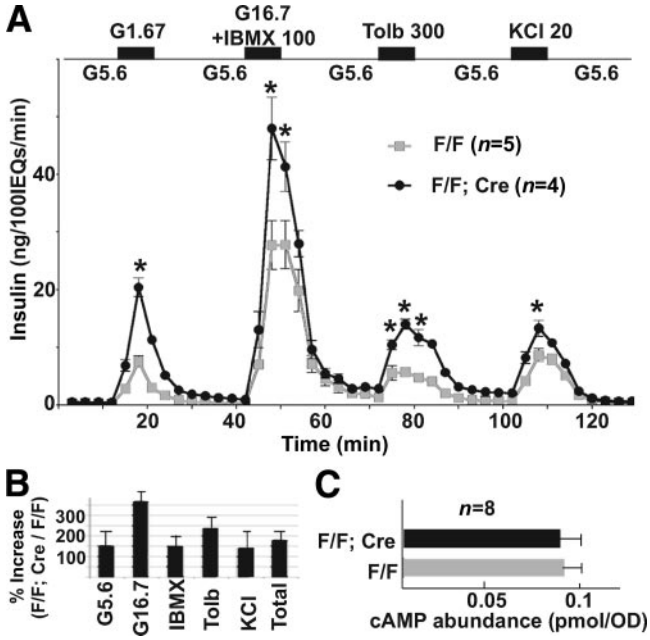

FIG. 4. *Gαo* nullizygous islets secrete more insulin in response to multiple stimulations. *A*: Perifusion assay results. Note the enhanced insulin secretion response to different secretagogues. IEQ = islet equivalent. *$P < 0.01$. *B*: Total insulin release induced by different secretagogues. Data are integrated from *A*. *C*: cAMP levels in mutant and control islets. The cAMP concentration is normalized against the OD280 of islet extract (as an assay of protein content).

Synchronous bursting and spiking activities were observed at 8, 10, and 15 mmol/l glucose, respectively (Fig. 5*A* and data not shown), in both sets of islets. The mean fold increase in $[Ca^{2+}]_i$ was also similar for various levels of glucose stimulation for both mutant and wild-type islets (Fig. 5*B*). This result suggests that Gαo has little effect on β-cell electrical activity and suggests that Gαo regulates insulin secretion downstream of elevated $[Ca^{2+}]_i$ in vivo.

Gαo inhibits insulin granule docking to the β-cell plasma membrane. We next examined how Gαo affects insulin secretion. Because insulin vesicle docking on the cell membrane is necessary for insulin secretion, we used TEM to investigate whether vesicle distribution in β-cells is affected by loss of *Gαo*. The size of each vesicle in β-cells did not vary between *F/F;Cre* and *F/F* control islets (Fig. 6*A* and *B*). The density of granules in the *F/F;Cre* and control β-cell remained unchanged as well (Fig. 6*E*). However, the number of secretory vesicles in direct contact with the cell membrane increased by about 100% in *F/F;Cre* β-cells as compared with that of controls (Fig. 6*C*, *D*, and *F*). Because TEM only allows us to examine vesicle docking on a thin section with limited depth, we used TIRFM to verify the above findings. TIRFM uses evanescent light waves to selectively illuminate the β-cell surface at a 100-nm depth. Thus, this technique allows us to exclusively visualize the granules that localize in the proximity of the cell membrane on a wide cell surface area. Isolated islet cells were fixed and stained with insulin antibodies and subjected to TIRFM (Fig. 6*G*). Consistent with the above TEM-based finding, we observed a significant ($P < 0.01$) increase in the number of insulin vesicles close to plasma membrane in *Gαo* mutants (257/μm^2) over that of the control cells (190/μm^2) (Fig. 6*F*). Note that the fold increase of docked vesicles revealed by TIRFM (a 35% increase) is lower than that observed from TEM-based analysis (100% increase). This is an expected result be-

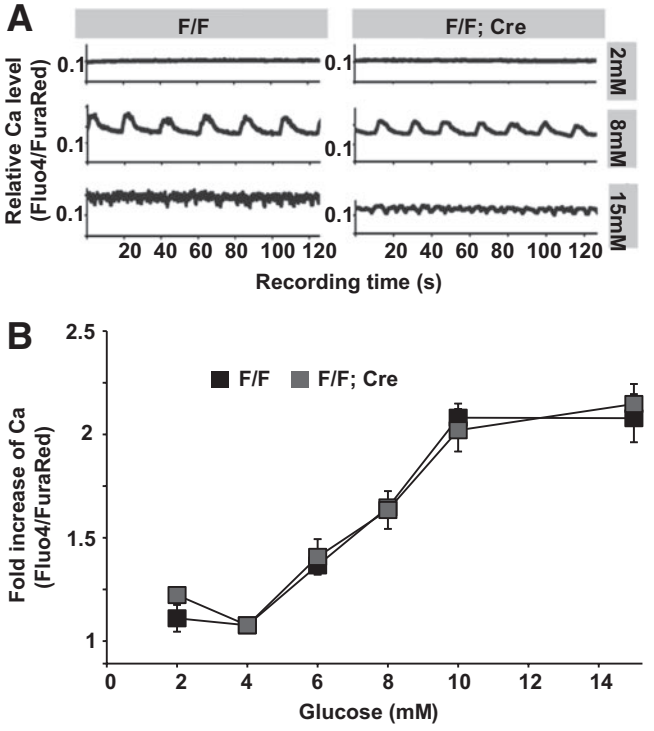

FIG. 5. Calcium responses were not altered in *Gαo* mutant islets. *A*: Representative time courses of $[Ca^{2+}]_i$ activity estimated from the normalized Fluo4/FuraRed intensity ratio in both *F/F* (*left*) and *F/F; Cre* islets (*right*) 10 min after glucose challenge. Shown are data from representative islets. Each islet was monitored continuously for 2 min. Note that 2 mmol/l glucose does not elicit Ca^{2+} mobilization, whereas 8 mmol/l glucose induces synchronous bursting of Ca^{2+} activity in both sets of islets; 15 mmol/l glucose induces continuous spiking in both sets of islets. *B*: Fold increases in $[Ca^{2+}]_i$ estimated from the normalized Fluo4/FuraRed intensity ratio for control islets (*black*) and mutant islets (*gray*) under varying glucose stimulation. All data are normalized to Fluo4/FuraRed intensity ratio at 4 mmol/l glucose.

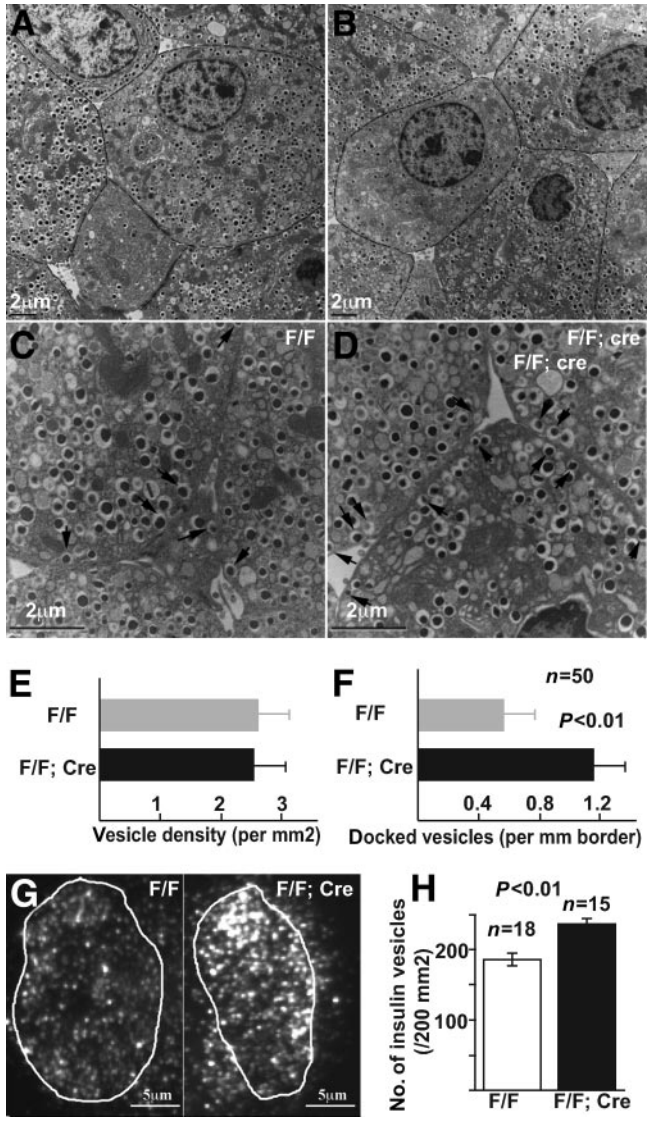

FIG. 6. *Gαo* inactivation increases insulin vesicle docking to β-cell membrane. *A–D*: TEM images highlighting insulin vesicle density (*A* and *B*). Note that different β-cells have different vesicle density or membrane-associated vesicles (*C* and *D*). Arrows, membrane-docked vesicles. *E*: Vesicle density in β-cells, presented as number of vesicles on two-dimensional views. *F*: Number of vesicles docked onto cytoplasmic membrane from EM-based analysis. Data are presented as number of vesicles over length of intercellular junctions ($P < 0.01$). *G*: TIRFM images showing the presence of insulin vesicles on the surface of fixed and insulin Ab-stained β-cells of control (*F/F*) and *Gαo* deleted (*F/F; Cre*) animals. Vesicles within the circled areas were counted and presented in *H*.

cause TEM identifies the vesicles that directly contact the plasma membrane, which is only a small portion of the vesicles that localize within 100 nm of the plasma membrane visualized through TIRFM. Additionally, our vesicle density count with EM and TIRFM displayed a twofold difference (Fig. 6*E* and *H*). This discrepancy could be due to the unequal vesicle distribution within the cytoplasmic compartment and cell membrane. Alternatively, it is possible that TIRFM only visualizes high-insulin-content vesicles (due to antibody staining–related issues), whereas EM allows us to visualize all vesicles.

***Gαo* inactivation expedites vesicle release in β-cells but does not affect vesicle trafficking from cytoplasm to plasma membrane.** TIRFM visualizes vesicle movement in vivo in real time. We therefore recorded the vesicular dynamics close to the β-cell membrane in wild-type and *Gαo* mutant animals. Dissociated β-cells were transfected with retroviral particles that expressed a human insulin–enhanced green fluorescent protein (EGFP) fusion protein, which was previously shown to be packaged in normal insulin vesicles and to not interfere with insulin trafficking. As a result, the EGFP-marked insulin vesicles could be followed in real time (29,37).

Islet cells were stimulated with 22 mmol/l glucose (see RESEARCH DESIGN AND METHODS). Vesicular movements close to the β-cell membrane were recorded at 300-ms intervals with TIRFM. The number of fusion events at the plasma membrane was counted at 1-min intervals. Consistent with the perifusion assays (Fig. 4), *Gαo* mutant β-cells release significantly more vesicles than control β-cells (Fig. 7*A*). In this regard, it is possible that *Gαo* inactivation could either shorten vesicle residence time on the plasma membrane before fusion or expedite transportation of vesicles from cytoplasm to plasma membrane. In order to differentiate between these possibilities, we counted the fusion events from predocked vesicles and newly arrived vesicles (newcomers or vesicles that appear close to cell membranes after the start of recording) during stimulation. Membrane-docked vesicles in *Gαo* mutant β-cells showed a trend of increased readiness for release (Fig. 7*B*). Specifically, upon glucose stimulation, 23.1% of predocked insulin vesicles were released within 10 min in control β-cells, whereas 35.7% of predocked vesicles were released within

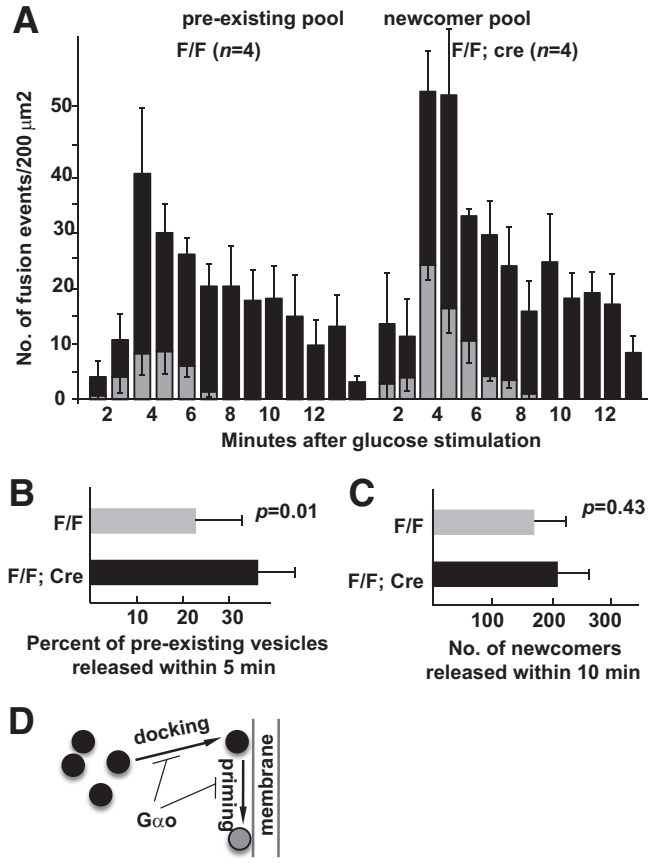

FIG. 7. *Gαo*$^{-/-}$ cells release insulin vesicles more readily upon glucose stimulation. *A*: The numbers of vesicle–plasma membrane fusion events at several time points with 22 mmol/l glucose stimulation. The events are presented as fusions from predocked vesicles and fusions from newly arrived vesicles, respectively. *B*: The percent of predocked vesicles that are released within 10 min of glucose stimulation. *C*: The number of newly arrived vesicles that are released within 10 min of glucose induction. *D*: A simple model summarizing where Gαo could exert its function in the vesicle-secretion process, including vesicle docking and possibly priming.

the same time frame in β-cells without *Gαo* (Fig. 7*B*); this represents a 52% increase. On the contrary, the fusion events contributed by newly arrived vesicles did not display a significant difference between the control and mutant β-cells (Fig. 7*C*, 174 ± 58 vs. 213 ± 68; <23% difference). Overall, these data suggest that one of the possible *Gαo* functions is to facilitate vesicle docking and, to a lesser extent, to increase the readiness of vesicle fusion to the plasma membrane (Fig. 7*D*).

DISCUSSION

Although the role of *Gαo* in insulin secretion has been implicated for one-half century from PTX-based G-protein uncoupling studies (11–13), the nonspecificity of PTX (which inactivates both Gαi and Gαo) has made it impossible to investigate how Gαo functions in vivo. Our findings suggest that Gαo might regulate insulin granule dynamics distal to Ca^{2+} mobilization in vivo, a conclusion drawn from cell culture–based studies (38–42).

Vesicle docking is an essential step for insulin secretion. Each β-cell contains more than 10,000 vesicles (43,44), yet only a small portion of these vesicles can be readily released within the first phase of glucose induction (<10 min in all studied species) (2,7). Subsequently, insulin vesicles are transported from cytoplasm to the plasma membrane for docking, priming, and fusion to sustain the second phase of release. Thus, vesicle docking, although not the rate-limiting step for insulin secretion, likely plays an essential role in regulating insulin secretion. Consistent with this hypothesis, adult β-cells that have lost the transcription factor gene *FoxA2* have more insulin vesicles docked on the cell membrane, and this phenotype is accompanied by excessive glucose-stimulated insulin secretion (45). Thus, understanding vesicle trafficking could provide key insights into the mechanisms that regulate insulin release in response to nutritional, neuronal, and hormonal stimuli.

Both our TEM- and TIRFM-based studies show that loss of *Gαo* results in more vesicles docking to the plasma membrane at the resting state. Furthermore, the docked vesicles in *Gαo* nullizygous β-cells appear more likely to fuse with the plasma membrane than docked vesicles in control cells. These data, combined with the finding that *Gαo* inactivation does not significantly alter the transport of vesicles to plasma membrane, suggest that Gαo could delay vesicle docking and possibly repress vesicle priming. Further supporting this notion is our finding that Gαo does not appear to affect calcium flux, which seems to contradict some previously published findings (10). It is likely that only specific G-protein (Gαβγ)-coupled receptor–ligand coupling could affect channel activity via Gαo, which cannot be activated in our in vitro assay. Alternatively, the in vitro assays may not be sensitive enough to detect the subtle channel activity alteration with or without Gαo. For example, Gαo could regulate the resting Ca^{2+} levels in β-cells, which would be consistent with the finding that resting Ca^{2+} level affects the pool size of readily releasable granules (46). It would be interesting to analyze whether hormones, such as galanin, somatostatin, or adrenaline, can regulate specific channel activities in the presence or absence of Gαo and how this might affect the resting Ca^{2+} levels in isolated islets.

How Gαo modulates the vesicle docking/priming process is not known. Because there are high levels of Gαo protein in neuronal and neuroendocrine cells, it was proposed that one function of Gαo was to act as a reservoir for the Gβγ subunits within cells. When stimulated, Gαo will dissociate from the Gαβγ to release Gβγ as an effector to regulate cell function. Several lines of existing evidence support this possibility. First, expressing a Gβγ binding protein, the PH domain of the G-protein–linked receptor kinase 2 stimulates insulin secretion in response to secretagogues, similar to the consequences of Gαβγ trimer formation (47). Second, introducing Gβγ proteins in neuronal cells mimics the effect of Gαo protein activation, that is, dissociation of the Gαβγ complex (48). In line with this possibility, loss of Gαo could reduce cellular Gβγ subunits, which results in dysregulated vesicle trafficking and secretion (17). Unfortunately, it is currently unknown which specific β- or γ-subunit interacts with Gαo and has thus prevented us from directly examining this possibility. Alternatively, Gαo proteins could directly interact with unknown effectors to regulate insulin secretion. Solving this issue will likely require a comprehensive understanding of all the protein/effectors that specifically interact with Gαo under normal physiological conditions. We currently do not know which possibility is likely to occur.

In summary, our analysis suggests that Gαo modulates insulin secretion by regulating vesicle docking on the β-cell membrane. Addressing the specific mechanism

likely requires a comprehensive analysis of proteins that interact with Gαo and how these proteins modulate vesicle trafficking, docking, priming, and fusion processes.

ACKNOWLEDGMENTS

This research was supported by grants from the National Institutes of Health (DK-069771 to M.J., DK-53434 to D.P.), JDRF (2009-371 to G.G.), and by the Intramural Research Program of the National Institutes of Health (Z01-ES-101643 to L.B.). A.C.P. was supported by grants from the JDRF, the VA Research Service, the National Institutes of Health (DK-66636, DK-69603, and DK-63439), the Vanderbilt Mouse Metabolic Phenotyping Center (DK-59637), and the Vanderbilt Diabetes Research and Training Center (DK-20593). S.N. was supported by the following resource: KAKENHI (C-20570189, 21113523 to M.O.-I., B-20390260 to S.N.), Sumitomo Foundation (to M.O.-I.), Astellas Foundation for Research on Metabolic Disorders (M.O.-I.), and Research Foundation for Opto-Science and Technology (M.O.-I.). TEM was performed in the Vanderbilt EM core facility, with help from Denny Kerns, Matt Stephenson, and Mary Dawes. The color print fee cost was covered by JDRF.

No potential conflicts of interest relevant to this article were reported.

A.Z., Y.X., Y.H., J.A., and G.B. contributed research data. G.G. contributed research data and wrote the manuscript. M.O.-I., M.B., R.K.P.B., and S.N. contributed research data and manuscript editing. A.C.P., M.J., D.P., and L.B. contributed to discussion and edited the manuscript.

We thank Ethan Lee and Lindsay Bramson from the Vanderbilt Medical Center, Cell and Developmental Biology, for help with preparing the manuscript. We are grateful to R. Jahn (Max Plank Institute, Munich, Germany) for providing the Gαo antibody.

REFERENCES

1. Matschinsky FM. Glucokinase as glucose sensor and metabolic signal generator in pancreatic beta-cells and hepatocytes. Diabetes 1990;39:647–652
2. Bratanova-Tochkova TK, Cheng H, Daniel S, Gunawardana S, Liu Y-J, Mulvaney-Musa J, Schermerhorn T, Straub SG, Yajima H, Sharp GWG. Triggering and augmentation mechanisms, granule pools, and biphasic insulin secretion. Diabetes 2002;51(Suppl. 1):S83–S90
3. Matthews DR, Clark A. Neural control of the endocrine pancreas. Proc Nutr Soc 1987;46:89–95
4. Lang J. Molecular mechanisms and regulation of insulin exocytosis as a paradigm of endocrine secretion. Eur J Biochem 1999;259:3–17
5. Henquin JC. Triggering and amplifying pathways of regulation of insulin secretion by glucose. Diabetes 2000;49:1751–1760
6. Ahrén B. Autonomic regulation of islet hormone secretion: implications for health and disease. Diabetologia 2000;43:393–410
7. Rorsman P, Renström E. Insulin granule dynamics in pancreatic beta cells. Diabetologia 2003;46:1029–1045
8. Birnbaumer L. Receptor-to-effector signaling through G proteins: roles for beta gamma dimers as well as alpha subunits. Cell 1992;71:1069–1072
9. Birnbaumer L. Expansion of signal transduction by G proteins. The second 15 years or so: from 3 to 16 alpha subunits plus betagamma dimers. Biochim Biophys Acta 2007;1768:772–793
10. Sharp GW. Mechanisms of inhibition of insulin release. Am J Physiol 1996;271:C1781–C1799
11. Gulbenkian A, Schobert L, Nixon C, Tabachnick IIA. Metabolic effects of pertussis sensitization in mice and rats. Endocrinology 1968;83:885–892
12. Szentivanyi A, Fishel CW, Talmage DW. Adrenaline mediation of histamine and serotonin hyperglycemia in normal mice and the absence of adrenaline-induced hyperglycemia in pertussis-sensitized mice. J Infect Dis 1963;113:86–98
13. Yajima M, Hosoda K, Kanbayashi Y, Nakamura T, Nogimori K, Mizushima Y, Nakase Y, Ui M. Islets-activating protein (IAP) in Bordetella pertussis that potentiates insulin secretory responses of rats. Purification and characterization. J Biochem 1978;83:295–303
14. Regard JB, Kataoka H, Cano DA, Camerer E, Yin L, Zheng YW, Scanlan TS, Hebrok M, Coughlin SR. Probing cell type-specific functions of Gi in vivo identifies GPCR regulators of insulin secretion. J Clin Invest 2007;117:4034–4043
15. Hsu WH, Rudolph U, Sanford J, Bertrand P, Olate J, Nelson C, Moss LG, Boyd AE, Codina J, Birnbaumer L. Molecular cloning of a novel splice variant of the alpha subunit of the mammalian Go protein. J Biol Chem 1990;265:11220–11226
16. Strathmann M, Wilkie TM, Simon MI. Alternative splicing produces transcripts encoding two forms of the alpha subunit of GTP-binding protein Go. Proc Natl Acad Sci U S A 1990;87:6477–6481
17. Blackmer T, Larsen EC, Bartleson C, Kowalchyk JA, Yoon EJ, Preininger AM, Alford S, Hamm HE, Martin TF. G protein betagamma directly regulates SNARE protein fusion machinery for secretory granule exocytosis. Nat Neurosci 2005;8:421–425
18. Gerachshenko T, Blackmer T, Yoon EJ, Bartleson C, Hamm HE, Alford S. Gbetagamma acts at the C terminus of SNAP-25 to mediate presynaptic inhibition. Nat Neurosci 2005;8:597–605
19. Wang Z, Thurmond DC. Mechanisms of biphasic insulin-granule exocytosis: roles of the cytoskeleton, small GTPases and SNARE proteins. J Cell Sci 2009;122:893–903
20. Jiang M, Gold MS, Boulay G, Spicher K, Peyton M, Brabet P, Srinivasan Y, Rudolph U, Ellison G, Birnbaumer L. Multiple neurological abnormalities in mice deficient in the G protein Go. Proc Natl Acad Sci U S A 1998;95:3269–3274
21. Valenzuela D, Han X, Mende U, Fankhauser C, Mashimo H, Huang P, Pfeffer J, Neer EJ, Fishman MC. G alpha(o) is necessary for muscarinic regulation of Ca2+ channels in mouse heart. Proc Natl Acad Sci U S A 1997;94:1727–1732
22. Gu G, Dubauskaite J, Melton DA. Direct evidence for the pancreatic lineage: NGN3+ cells are islet progenitors and are distinct from duct progenitors. Development 2002;129:2447–2457
23. Winter S, Brunk I, Walther DJ, Höltje M, Jiang M, Peter JU, Takamori S, Jahn R, Birnbaumer L, Ahnert-Hilger G. Galphao2 regulates vesicular glutamate transporter activity by changing its chloride dependence. J Neurosci 2005;25:4672–4680
24. Zhang MZ, Wang JL, Cheng HF, Harris RC, McKanna JA. Cyclooxygenase-2 in rat nephron development. Am J Physiol 1997;273:F994–F1002
25. Wang S, Zhang J, Zhao A, Hipkens S, Magnuson MA, Gu G. Loss of Myt1 function partially compromises endocrine islet cell differentiation and pancreatic physiological function in the mouse. Mech Dev 2007;124:898–910
26. Komatsu M, McDermott AM, Gillison SL, Sharp GW. Time course of action of pertussis toxin to block the inhibition of stimulated insulin release by norepinephrine. Endocrinology 1995;136:1857–1863
27. Brissova M, Shiota M, Nicholson WE, Gannon M, Knobel SM, Piston DW, Wright CV, Powers AC. Reduction in pancreatic transcription factor PDX-1 impairs glucose-stimulated insulin secretion. J Biol Chem 2002;277:11225–11232
28. Rocheleau JV, Remedi MS, Granada B, Head WS, Koster JC, Nichols CG, Piston DW. Critical role of gap junction coupled KATP channel activity for regulated insulin secretion. PLoS Biol 2006;4:e26
29. Ohara-Imaizumi M, Nishiwaki C, Kikuta T, Nagai S, Nakamichi Y, Nagamatsu S. TIRF imaging of docking and fusion of single insulin granule motion in primary rat pancreatic beta-cells: different behaviour of granule motion between normal and Goto-Kakizaki diabetic rat beta-cells. Biochem J 2004;381:13–18
30. Ohara-Imaizumi M, Fujiwara T, Nakamichi Y, Okamura T, Akimoto Y, Kawai J, Matsushima S, Kawakami H, Watanabe T, Akagawa K, Nagamatsu S. Imaging analysis reveals mechanistic differences between first- and second-phase insulin exocytosis. J Cell Biol 2007;177:695–705
31. Zenisek D, Steyer JA, Almers W. Transport, capture and exocytosis of single synaptic vesicles at active zones. Nature 2000;406:849–854
32. Gu G, Wells JM, Dombkowski D, Preffer F, Aronow B, Melton DA. Global expression analysis of gene regulatory pathways during endocrine pancreatic development. Development 2004;131:165–179
33. Katada T, Ui M. Direct modification of the membrane adenylate cyclase system by islet-activating protein due to ADP-ribosylation of a membrane protein. Proc Natl Acad Sci U S A 1982;79:3129–3133
34. Katada T, Ui M. ADP ribosylation of the specific membrane protein of C6 cells by islet-activating protein associated with modification of adenylate cyclase activity. J Biol Chem 1982;257:7210–7216
35. Renström E, Eliasson L, Rorsman P. Protein kinase A-dependent and -independent stimulation of exocytosis by cAMP in mouse pancreatic B-cells. J Physiol 1997;502:105–118

36. Ozaki N, Shibasaki T, Kashima Y, Miki T, Takahashi K, Ueno H, Sunaga Y, Yano H, Matsuura Y, Iwanaga T, Takai Y, Seino S. cAMP-GEFII is a direct target of cAMP in regulated exocytosis. Nat Cell Biol 2000;2:805–811
37. Ohara-Imaizumi M, Nakamichi Y, Nishiwaki C, Nagamatsu S. Transduction of MIN6 beta cells with TAT-syntaxin SNARE motif inhibits insulin exocytosis in biphasic insulin release in a distinct mechanism analyzed by evanescent wave microscopy. J Biol Chem 2002;277:50805–50811
38. Abel KB, Lehr S, Ullrich S. Adrenaline-, not somatostatin-induced hyperpolarization is accompanied by a sustained inhibition of insulin secretion in INS-1 cells. Activation of sulphonylurea K+ATP channels is not involved. Pflugers Arch 1996;432:89–96
39. Ullrich S, Prentki M, Wollheim CB. Somatostatin inhibition of Ca2(+)-induced insulin secretion in permeabilized HIT-T15 cells. Biochem J 1990;270:273–276
40. Ullrich S, Wollheim CB. GTP-dependent inhibition of insulin secretion by epinephrine in permeabilized RINm5F cells. Lack of correlation between insulin secretion and cyclic AMP levels. J Biol Chem 1988;263:8615–8620
41. Wollheim CB, Winiger BP, Ullrich S, Wuarin F, Schlegel W. Somatostatin inhibition of hormone release: effects on cytosolic Ca++ and interference with distal secretory events. Metabolism 1990;39(Suppl. 2):101–104
42. Lang J, Nishimoto I, Okamoto T, Regazzi R, Kiraly C, Weller U, Wollheim CB. Direct control of exocytosis by receptor-mediated activation of the heterotrimeric GTPases Gi and G(o) or by the expression of their active G alpha subunits. EMBO J 1995;14:3635–3644
43. Dean PM. Ultrastructural morphometry of the pancreatic -cell. Diabetologia 1973;9:115–119
44. Olofsson CS, Göpel SO, Barg S, Galvanovskis J, Ma X, Salehi A, Rorsman P, Eliasson L. Fast insulin secretion reflects exocytosis of docked granules in mouse pancreatic B-cells. Pflugers Arch 2002;444:43–51
45. Gao N, White P, Doliba N, Golson ML, Matschinsky FM, Kaestner KH. Foxa2 controls vesicle docking and insulin secretion in mature beta cells. Cell Metab 2007;6:267–279
46. Gromada J, Høy M, Renström E, Bokvist K, Eliasson L, Göpel S, Rorsman P. CaM kinase II-dependent mobilization of secretory granules underlies acetylcholine-induced stimulation of exocytosis in mouse pancreatic B-cells. J Physiol 1999;518:745–759
47. Zhang H, Yasrebi-Nejad H, Lang J. G-protein betagamma-binding domains regulate insulin exocytosis in clonal pancreatic beta-cells. FEBS Lett 1998;424:202–206
48. Blackmer T, Larsen EC, Takahashi M, Martin TF, Alford S, Hamm HE. G protein betagamma subunit-mediated presynaptic inhibition: regulation of exocytotic fusion downstream of Ca2+ entry. Science 2001;292:293–297